Inorganic Chemistry

ARTICLE

pubs.acs.org/IC

Homochiral Frameworks Formed by Reactions of Lanthanide Ions with a Chiral Antimony Tartrate Secondary Building Unit

Qiang Gao, Xiqu Wang, and Allan J. Jacobson*

Department of Chemistry, University of Houston, Houston, Texas 77204-5003, United States

Supporting Information

ABSTRACT: A chiral cluster compound, dipotassium bis(μ-tartrato)diantimony(III), $K_2Sb_2L_2$ (H_4L = L-tartaric acid), was used as a secondary building unit to react with lanthanide ions. Three series of homochiral coordination compounds were obtained: 0D $[La(H_2L)(H_2O)_4]_2[Sb_2L_2]\cdot 7H_2O$ (**0D-La**), 1D $Ln(Sb_2L_2)(H_2O)_5(NO_3)\cdot H_2O$ (**1D-Ln**) (Ln = La−Lu or Y, expect Pm), 2D(I) $[(Ln(H_2O)_5)_2(Sb_2L_2)_3]\cdot 5H_2O$ (**2D(I)-Ln**) (Ln = La, Ce, Pr), and 2D(II) $[(La(H_2O)_5)_2(Sb_2L_2)_3]\cdot 6H_2O$ (**2D(II)-La**). Single-crystal X-ray diffraction studies indicated that **0D-La** crystallizes in space group $P1$, and the structure contains isolated $Sb_2L_2^{2-}$ units located between chains of composition $La(H_2L)(H_2O)_4$. The series of **1D-Ln** compounds is isostructural and crystallizes in space group $P2_12_12_1$. In the structure, $Sb_2L_2^{2-}$ units are coordinated to two Ln ions by two out of the four free tartrate oxygen atoms to form a linear chain. To the best of our knowledge, this is the first example of a homochiral structure that can be formed for the whole lanthanide series. In the **2D(I)-Ln** structure series, which crystallizes in space group $P2_1$, the $Sb_2L_2^{2-}$ units have two distinct coordination modes: one is the same as that found in the 1D structure, while in the other all four free tartrate oxygen atoms are coordinated to four Ln ions in a very distorted tetrahedral arrangement. The connectivity between $Sb_2L_2^{2-}$ secondary units and LnO_9 polyhedra gives rise to infinite layers. 2D(II) $[(La(H_2O)_5)_2(Sb_2L_2)_3]\cdot 6H_2O$, which crystallizes in space group $C2$, has a similar network to the **2D(I)-Ln** compounds. The trends in lattice parameters, bond lengths, and ionic radii in the **1D-Ln** series were analyzed to show the effect of the lanthanide contraction.

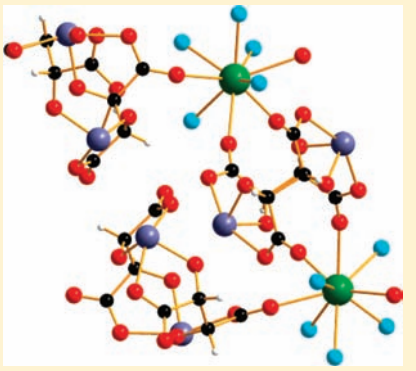

INTRODUCTION

Metal−organic frameworks (MOFs) have been investigated in recent years because of their intriguing topologies and potential applications in fields such as gas adsorption and separation,[1] catalysis,[2] magnetism,[3] and luminescence.[4] Structural details, such as pore dimensions and the number of interpenetrated lattices, can be manipulated by varying metal centers and the linking organic ligands.[5] Among the various metal ions that have been investigated, lanthanide ions have attracted significant attention because of their characteristic optical, magnetic, and catalytic properties[6] and because the high coordination numbers of lanthanide ions results in structural diversity and unusual architectures not observed for d-block transition metal compounds.[7]

As part of the general study of MOFs, the synthesis of homochiral compounds is of particular interest because of the potential for important applications in enantioselectivity and chiral catalysis.[8] Moreover, they may show some intriguing physical properties such as second-harmonic generation (SHG) and ferroelectricity.[9] Three distinct approaches have been exploited: (1) use of chiral bridging ligands to connect metal ions or secondary building units,[10] (2) use of chiral coligands (templates) that do not participate in the framework but direct formation of a chiral structure,[11] and (3) use of achiral ligands that crystallize in chiral space groups.[12] Among these three strategies, the first one provides the most straightforward and reliable way to synthesize homochiral MOFs. Coumpounds formed by enaniomerically pure D- or L- tartrate are illustrative of this approach.[13] Cheetham et al. studied the diversity of structures formed by alkali and alkaline earth metal tartrates and their relative stabilities.[13a−c] Tartrate compounds with d-block metal ions have also been reported.[13d−i] The framework structures of tartrates with different metal ions and ancillary ligands are very different, but many of them contain a common building unit containing two tartrate ligands and two metal ions connected to form a dimer in which each metal ion is bonded to four oxygen atoms from the two tartrate groups.

We are interested in one well-known chiral tartrate dimer $K_2Sb_2L_2$ (H_4L = L-tartaric acid), namely, dipotassium bis(μ-tartrato)diantimony(III) ("tartar emetic").[14] In this dimer, each L-tartrate bridges two antimony(III) ions in a chelating mode with two oxygen atoms from two carboxylate groups and another two from the hydroxyl groups. Each Sb^{3+} ion is four coordinated, with the electron lone pairs pointing outward. Thus, the ligand possesses four uncoordinated oxygen atoms arranged in a highly distorted tetrahedral motif (Figure S1, Supporting Information).

Here, we report three types of homochiral coordination compounds prepared by reactions of $Sb_2L_2^{2-}$ as a secondary building unit with lanthanide ions: 0D $[La(H_2L)(H_2O)_4]_2[Sb_2L_2]\cdot 7H_2O$ (**0D-La**), 1D $Ln(Sb_2L_2)(H_2O)_5(NO_3)\cdot H_2O$ (**1D-Ln**) (Ln = La−Lu or Y, expect Pm), 2D(I) $[(Ln(H_2O)_5)_2(Sb_2L_2)_3]\cdot 5H_2O$ (Ln = La, Ce, Pr) (**2D(I)-Ln**), and 2D(II) $[(La(H_2O)_5)_2(Sb_2L_2)_3]\cdot 6H_2O$ (**2D(II)-La**). Single-crystal X-ray

Received: June 13, 2011
Published: August 22, 2011

Table 1. Crystal Data for All Compounds

	0D-La	1D-La	1D-Ce	1D-Pr	1D-Nd	1D-Sm	1D-Eu
empirical formula	$C_{16}H_{38}La_2O_{39}Sb_2$	$C_8H_{16}LaNO_{21}Sb_2$	$C_8H_{16}CeNO_{21}Sb_2$	$C_8H_{16}PrNO_{21}Sb_2$	$C_8H_{16}NdNO_{21}Sb_2$	$C_8H_{16}SmNO_{21}Sb_2$	$C_8H_{16}EuNO_{21}Sb_2$
fw	1375.78	844.63	845.84	846.63	849.96	856.07	857.68
cryst appearance	colorless needle	colorless plate	colorless plate	green plate	pink plate	colorless plate	colorless plate
cryst size, mm	0.2 × 0.05 × 0.05	0.24 × 0.15 × 0.08	0.22 × 0.12 × 0.06	0.20 × 0.12 × 0.06	0.24 × 0.12 × 0.06	0.20 × 0.12 × 0.05	0.20 × 0.10 × 0.05
cryst syst	triclinic	orthorhombic	orthorhombic	orthorhombic	orthorhombic	orthorhombic	orthorhombic
space group	$P1$	$P2_12_12_1$	$P2_12_12_1$	$P2_12_12_1$	$P2_12_12_1$	$P2_12_12_1$	$P2_12_12_1$
a (Å)	8.059(2)	10.3132(3)	10.3057(3)	10.3041(5)	10.2946(3)	10.2895(3)	10.2745(3)
b (Å)	8.180(2)	11.3906(4)	11.3715(4)	11.3683(5)	11.3515(4)	11.3299(4)	11.3155(4)
c (Å)	14.813(4)	17.1833(6)	17.1293(6)	17.0918(8)	17.0396(6)	16.9699(6)	16.9122(6)
α (deg)	98.870(3)	90.0	90.0	90.0	90.0	90.0	90.0
β (deg)	99.255(3)	90.0	90.0	90.0	90.0	90.0	90.0
γ (deg)	90.596(3)	90.0	90.0	90.0	90.0	90.0	90.0
V (Å^3)	951.7(4)	2018.58(12)	2007.40(12)	2002.14(16)	1991.23(11)	1978.33(11)	1966.23(11)
Z	1	4	4	4	4	4	4
μ (mm^{-1})	3.732	4.844	5.010	5.183	5.372	5.751	5.990
θ range for data collection (deg)	2.52−28.27	2.15−28.25	2.15−28.31	2.15−28.38	2.16−29.78	2.16−28.32	2.17−28.29
calcd density (g/cm^3)	2.401	2.779	2.799	2.809	2.835	2.874	2.897
F_{000}	662	1592	1596	1600	1604	1612	1616
reflns collected	5775	12 236	12 724	12 101	13 105	12 619	12 426
unique reflns	5775	4785	4804	4761	5025	4554	4709
R_{int}	0.0266	0.0381	0.0213	0.0271	0.0349	0.0463	0.0557
parameters/restraints	258/3	298/0	298/0	298/0	298/0	298/0	298/0
Flack x	0.02(2)	−0.038(17)	−0.003(11)	−0.015(11)	−0.021(13)	−0.010(9)	−0.004(10)
goodness-of-fit on F^2	1.015	0.970	1.137	1.076	1.002	1.052	1.070
final R indices $[I > 2\sigma(I)]$	R_1 = 0.0387 wR_2 = 0.0938	R_1 = 0.0259 wR_2 = 0.0518	R_1 = 0.0169 wR_2 = 0.0472	R_1 = 0.0189 wR_2 = 0.0495	R_1 = 0.0261 wR_2 = 0.0578	R_1 = 0.0205 wR_2 = 0.0540	R_1 = 0.0263 wR_2 = 0.0683
R indices (all data)	R_1 = 0.0420 wR_2 = 0.0964	R_1 = 0.0301 wR_2 = 0.0530	R_1 = 0.0170 wR_2 = 0.0473	R_1 = 0.0204, wR_2 = 0.0501	R_1 = 0.0285 wR_2 = 0.0586	R_1 = 0.0212 wR_2 = 0.0543	R_1 = 0.0265 wR_2 = 0.0685
largest diff. peak and hole	1.337 and −1.036 e·A^{-3}	0.642 and −0.809 e·A^{-3}	0.608 and −1.275 e·A^{-3}	0.740 and −0.574 e·A^{-3}	1.658 and −1.235 e·A^{-3}	1.510 and −1.230 e·A^{-3}	0.724 and −1.704 e·A^{-3}

	1D-Gd	1D-Tb	1D-Dy	1D-Ho	1D-Er	1D-Tm	1D-Yb
empirical formula	$C_8H_{16}GdNO_{21}Sb_2$	$C_8H_{16}TbNO_{21}Sb_2$	$C_8H_{16}DyNO_{21}Sb_2$	$C_8H_{16}HoNO_{21}Sb_2$	$C_8H_{16}ErNO_{21}Sb_2$	$C_8H_{16}TmNO_{21}Sb_2$	$C_8H_{16}YbNO_{21}Sb_2$
fw	862.97	864.64	868.22	870.65	872.98	874.65	878.76
cryst appearance	colorless plate	colorless plate	colorless plate	red plate	red plate	colorless needle	colorless needle
cryst size, mm	0.20 × 0.12 × 0.06	0.20 × 0.10 × 0.04	0.18 × 0.08 × 0.04	0.20 × 0.10 × 0.04	0.20 × 0.10 × 0.04	0.16 × 0.06 × 0.06	0.15 × 0.06 × 0.06
cryst syst	orthorhombic	orthorhombic	orthorhombic	orthorhombic	orthorhombic	orthorhombic	orthorhombic
space group	$P2_12_12_1$	$P2_12_12_1$	$P2_12_12_1$	$P2_12_12_1$	$P2_12_12_1$	$P2_12_12_1$	$P2_12_12_1$
a (Å)	10.2741(4)	10.2675(3)	10.2594(3)	10.2606(3)	10.2617(3)	10.2590(3)	10.2511(3)
b (Å)	11.3121(4)	11.2978(4)	11.2855(4)	11.2852(4)	11.2688(4)	11.2557(4)	11.2635(4)
c (Å)	16.8856(6)	16.8401(6)	16.7969(6)	16.7766(5)	16.7347(6)	16.6920(6)	16.6615(6)
α (deg)	90.00	90.0	90.0	90.0	90.0	90.0	90.0
β (deg)	90.00	90.0	90.0	90.0	90.0	90.0	90.0
γ (deg)	90.00	90.0	90.0	90.0	90.0	90.0	90.0
V (Å^3)	1962.47(12)	1953.45(11)	1944.79(11)	1942.61(11)	1935.15(11)	1927.46(11)	1923.79(11)
Z	4	4	4	4	4	4	4
μ (mm^{-1})	6.185	6.439	6.673	6.907	7.182	7.459	7.723
θ range for data collection (deg)	2.17−28.38	2.17−29.82	2.17−28.28	2.17−28.87	2.18−29.85	2.18−28.35	2.18−28.32
calcd density (g/cm^3)	2.921	2.940	2.965	2.977	2.996	3.014	3.034

dx.doi.org/10.1021/ic201274c |*Inorg. Chem.* 2011, 50, 9073–9082

Table 1. Continued

	1D-Gd	1D-Tb	1D-Dy	1D-Ho	1D-Er	1D-Tm	1D-Yb
F_{000}	1620	1624	1628	1632	1636	1640	1644
reflns collected	12 481	12 465	14 439	12 324	12 555	12 223	11 570
unique reflns	4364	4767	4656	4722	4629	4594	4591
R_{int}	0.0306	0.0456	0.0526	0.0383	0.0350	0.0294	0.0556
parameters/restraints	298/0	299/0	299/0	298/0	298/0	298/0	298/0
Flack x	−0.015(8)	0.008(7)	−0.008(7)	−0.001(6)	0.015(8)	−0.010(6)	−0.024(9)
goodness-of-fit on F^2	0.969	1.105	1.088	1.081	1.119	1.114	0.967
final R indices $[I > 2\sigma(I)]$	R_1 = 0.0183	R_1 = 0.0211	R_1 = 0.0215	R_1 = 0.0200	R_1 = 0.0295	R_1 = 0.0185	R_1 = 0.0265
	wR_2 = 0.0461	wR_2 = 0.0563	wR_2 = 0.0558	wR_2 = 0.0524	wR_2 = 0.0785	wR_2 = 0.0496	wR_2 = 0.0555
R indices (all data)	R_1 = 0.0194	R_1 = 0.0211	R_1 = 0.0218	R_1 = 0.0202	R_1 = 0.0297	R_1 = 0.0191	R_1 = 0.0295
	wR_2 = 0.0464	wR_2 = 0.0563	wR_2 = 0.0559	wR_2 = 0.0526	wR_2 = 0.0787	wR_2 = 0.0498	wR_2 = 0.0562
largest diff. peak and hole	0.761 and −0.651 e·A^{-3}	1.173 and −1.483 e·A^{-3}	1.005 and −1.407 e·A^{-3}	0.881 and −1.309 e·A^{-3}	1.304 and −2.195 e·A^{-3}	1.409 and −0.489 e·A^{-3}	0.926 and −1.185 e·A^{-3}

	1D-Lu	1D-Y	2D(I)-La	2D(I)-Ce	2D(I)-Pr	2D(II)-La
empirical formula	$C_8H_{16}LuN\ O_{21}Sb_2$	$C_8H_{16}YN\ O_{21}Sb_2$	$C_{24}H_{42}La_2\ O_{51}Sb_6$	$C_{24}H_{42}Ce_2\ O_{51}Sb_6$	$C_{24}H_{42}Pr_2\ O_{51}Sb_6$	$C_{12}H_{22}La\ O_{26}Sb_3$
fw	880.69	794.63	2154.90	2157.32	2158.90	1086.46
cryst appearance	colorless needle	colorless plate	colorless plate	colorless plate	green plate	colorless plate
cryst size, mm	0.16 × 0.05 × 0.05	0.20 × 0.12 × 0.05	0.18 × 0.12 × 0.08	0.18 × 0.12 × 0.06	0.20 × 0.12 × 0.06	0.18 × 0.10 × 0.06
cryst syst	orthorhombic	orthorhombic	monoclinic	monoclinic	monoclinic	monoclinic
space group	$P2_12_12_1$	$P2_12_12_1$	$P2_1$	$P2_1$	$P2_1$	$C2$
a (Å)	10.260(3)	10.2648(7)	8.4771(2)	8.475(3)	8.469(2)	22.7141(10)
b (Å)	11.279(3)	11.2869(8)	26.3184(6)	26.271(8)	26.300(7)	8.5147(4)
c (Å)	16.619(4)	16.7783(12)	12.1893(3)	12.204(4)	12.198(3)	14.0115(6)
α (deg)	90.0	90.0	90.0	90.0	90.0	90.0
β (deg)	90.0	90.0	109.68	110.32	110.31	105.659
γ (deg)	90.0	90.0	90.0	90.0	90.0	90.0
V (Å^3)	1923.2(8)	1943.9(2)	2560.55(11)	2548.0(13)	2548.1(11)	2609.3(2)
Z	4	4	2	2	2	4
μ (mm^{-1})	7.996	5.832	4.880	5.014	5.140	4.792
θ range for data collection (deg)	2.18−28.34	2.17−28.31	1.55−28.30	1.78−28.39	1.55−28.38	1.86−28.30
calcd density (g/cm^3)	3.042	2.715	2.795	2.812	2.814	2.766
F_{000}	1648	1520	2028	2032	2036	2048
reflns collected	12 111	10 281	16 103	15 325	15 550	8125
unique reflns	4629	4470	8571	9282	9686	5406
R_{int}	0.0766	0.0319	0.0189	0.0268	0.0317	0.0297
parameters/restraints	298/0	298/0	748/1	748/1	748/1	379/1
Flack x	−0.029(9)	−0.028(6)	0.001(9)	0.003(14)	0.006(12)	−0.01(2)
goodness-of-fit on F^2	0.924	0.935	1.087	1.034	1.003	1.010
final R indices $[I > 2\sigma(I)]$	R_1 = 0.0360	R_1 = 0.0252	R_1 = 0.0187	R_1 = 0.0269	R_1 = 0.0290	R_1 = 0.0325
	wR_2 = 0.0573	wR_2 = 0.0519	wR_2 = 0.496	wR_2 = 0.0731	wR_2 = 0.0745	wR_2 = 0.0805
R indices (all data)	R_1 = 0.0535	R_1 = 0.0308	R_1 = 0.0189	R_1 = 0.0286	R_1 = 0.0303	R_1 = 0.0337
	wR_2 = 0.0633	wR_2 = 0.0530	wR_2 = 0.0497	wR_2 = 0.0747	wR_2 = 0.0752	wR_2 = 0.0815
largest diff. peak and hole	1.190 and −0.858 e·A^{-3}	0.800 and −0.463 e·A^{-3}	0.745 and −0.897 e·A^{-3}	1.055 and −0.983 e·A^{-3}	1.483 and −1.000 e·A^{-3}	2.221 and −2.602 e·A^{-3}

diffraction studies indicated that **0D-La** crystallizes in space group $P1$, and the structure contains isolated $Sb_2L_2^{2-}$ dimers located between chains of composition $La(H_2L)(H_2O)_4$. The series of **1D-Ln** compounds is isostructural and crystallizes in space group $P2_12_12_1$. In the structure, $Sb_2L_2^{2-}$ units are coordinated to two Ln ions by two out of the four free tartrate oxygen atoms to form a linear chain. To the best of our knowledge, this is the first example of a homochiral structure that can be formed for the whole lanthanide series, while in the 2D structure series, which crystallize in space groups $P2_1$ or $C2$, $Sb_2L_2^{2-}$ units have two distinct coordination modes (one is the same as that found in the 1D structure, while in the other mode all of the four free tartrate oxygen atoms are coordinated to four Ln ions in a very distorted tetrahedral arrangement). The connectivity between $Sb_2L_2^{2-}$ secondary units and LnO_9 polyhedra gives rise to infinite layers. The compounds were characterized by infrared (IR), X-ray powder diffraction (XRD), thermogravimetric analyses (TGA), and photoluminescent studies. Second-order nonlinear measurements indicated that the

dx.doi.org/10.1021/ic201274c |*Inorg. Chem.* 2011, 50, 9073–9082

1D-Tb compound has a SHG efficiency that is comparable with α-quartz.

The synthesis of an isostructural series of compounds adds new data on complete series of structurally characterized lanthanide complexes for investigation of the lanthanide contraction and the monotonic shrinking of parameters such as bond distances over the 4f series.[15,16] The decrease in the magnitude of these parameters as a function of the number of 4f electrons can be well described by a second-order polynomial.[15a] The variation has been established by examination of isostructural series of lanthanide complexes published in the literature. Subsequently, this dependence has also been observed for a few other examples of incomplete series including solid-state materials as well as coordination complexes and has been successfully derived from a theoretical model.[15b,d] Later, Raymond et al. expanded the model and demonstrated a linear dependence of the inverse of the lanthanide ionic radius vs the number of f electrons.[15c] Because of the limited structural information available for complete isostructural series from La to Lu (excluding Pm), we analyzed the trends in lattice parameters and bond lengths for the **1D-Ln** series to discuss the effect of the lanthanide contraction.

EXPERIMENTAL SECTION

Materials and Methods. All of the reactants were reagent grade and were used as purchased without further purification. The IR spectra were measured on a Galaxy Series FTIR 5000 spectrometer with pressed KBr pellets. Thermogravimetric analysis (TGA) measurements were carried out using a TA Instruments Hi-Res 2950 system in N_2 flow with a heating rate of 3 °C min^{-1}. Elemental analyses were performed by Galbraith Laboratories (Knoxville, TN). The powder X-ray diffraction (XRD) patterns were collected at room temperature on a Phillps X'pert Pro diffractometer. Single-crystal X-ray analyses were performed on a Siemens SMART platform diffractometer outfitted with an Apex II area detector and monochromatized graphite Mo Kα radiation at room temperature (λ = 0.71013 Å). The structures were solved by direct methods and refined using SHELXTL.[17] Crystal data are summarized in Table 1. Fluorescence measurements were performed by using a PTI QuantaMaster QM4 CW Spectrofluorometer. Samples were confirmed by powder X-ray diffraction to be phase pure before measurements.

Preparation of $[La(H_2L)(H_2O)_4]_2[Sb_2L_2]\cdot 7H_2O$ (0D-La). An aqueous mixture (6.0 mL) containing $La(NO_3)_3\cdot 6H_2O$ (87.0 mg, 0.2 mmol), H_4L (30.0 mg, 0.2 mmol), and $K_2Sb_2L_2$ (62.0 mg, 0.1 mmol) with a pH ≈ 3 was placed in 16 mL vial; the vial was sealed, heated to 90 °C under autogenous pressure for 72 h, and then cooled to room temperature at ambient atmosphere. The product was washed with deionized water and dried in air. Colorless needle crystals of compound **0D-La** were obtained. Yield 30% based on $K_2Sb_2L_2$. Anal. Calcd for $C_{16}H_{38}La_2O_{39}Sb_2$: La, 20.19; Sb, 17.70; C, 13.97; H, 2.78. Found: La, 20.3; Sb, 17.5; C, 14.12; H, 2.86. IR (KBr): 3396(br. s), 1606(w), 1580(s), 1470(w), 1374(s), 1313(w), 1266(w), 1130(m), 1068(m), 895(w), 816 (w), 732(m), 640 (m).

Preparation of $La(Sb_2L_2)(H_2O)_5(NO_3)\cdot H_2O$ (1D-La). An aqueous mixture (5.0 mL) containing $La(NO_3)_3\cdot 6H_2O$ (87.0 mg, 0.2 mmol) and $K_2Sb_2L_2$ (123.0 mg, 0.2 mmol) with a pH ≈ 4 was placed in 16 mL vial; the vial was sealed, heated to 90 °C under autogenous pressure for 72 h, and then cooled to room temperature at ambient atmosphere. The product was washed with deionized water and dried in air. Colorless plate crystals of **1D-La** were obtained. Yield 40% based on $K_2Sb_2L_2$. Anal. Calcd for $C_8O_{21}Sb_2LaNH_{16}$: La, 16.4; Sb, 28.83; C, 11.38; H, 1.91; N, 1.66. Found: La, 15.6; Sb, 27.9; C, 11.32; H, 1.83; N, 1.61. IR (KBr): 3406(br. s), 1631(s), 1592(s), 1478(s), 1385(s), 1318(s), 1286(s), 1125(s), 1065(w), 891(m), 734(m).

Preparation of $Ce(Sb_2L_2)(H_2O)_5(NO_3)\cdot H_2O$ (1D-Ce). **1D-Ce** was synthesized in the same way as **1D-La** except that $Ce(NO_3)_3\cdot 6H_2O$ was used instead of $La(NO_3)_3\cdot 6H_2O$. A few colorless plate crystals of **1D-Ce** suitable for single-crystal X-ray diffraction were obtained.

Preparation of $Pr(Sb_2L_2)(H_2O)_5(NO_3)\cdot H_2O$ (1D-Pr). **1D-Pr** was synthesized in the same way as **1D-La** except that $Pr(NO_3)_3\cdot 6H_2O$ was used instead of $La(NO_3)_3\cdot 6H_2O$. Green plate crystals of **1D-Pr** were obtained. Yield 50% based on $K_2Sb_2L_2$. Anal. Calcd for $C_8O_{21}Sb_2PrNH_{16}$: Pr, 16.64; Sb, 28.76; C, 11.35; H, 1.90; N, 1.65. Found: Pr, 16.1; Sb, 29.4; C, 11.23; H, 1.85; N, 1.58. IR (KBr): 3380(br. s), 1632(s), 1594(s), 1477(s), 1386(s), 1320(s), 1288(s), 1125(s), 1069(m), 894(m), 738(s).

Preparation of $Nd(Sb_2L_2)(H_2O)_5(NO_3)\cdot H_2O$ (1D-Nd). **1D-Nd** was synthesized in the same way as **1D-La** except $Nd(NO_3)_3\cdot 6H_2O$ was used instead of $La(NO_3)_3\cdot 6H_2O$. Pink plate crystals of **1D-Nd** were obtained. Yield 48% based on $K_2Sb_2L_2$. Anal. Calcd for $C_8O_{21}Sb_2NdNH_{16}$: Nd, 16.97; Sb, 28.65; C, 11.30; H, 1.90; N, 1.65. Found: Nd, 15.7; Sb, 28.7; C, 11.88; H, 1.97; N, 1.61. IR (KBr): 3401(br. s), 1631(s), 1595(s), 1469(s), 1388(s), 1319(s), 1289(s), 1125(s), 1069(m), 894(m), 739(s).

Preparation of $Sm(Sb_2L_2)(H_2O)_5(NO_3)\cdot H_2O$ (1D-Sm). **1D-Sm** was synthesized in the same way as **1D-La** except that $Sm(NO_3)_3\cdot 6H_2O$ was used instead of $La(NO_3)_3\cdot 6H_2O$. Colorless plate crystals of **1D-Sm** were obtained. Yield 40% based on $K_2Sb_2L_2$. Anal. Calcd for $C_8O_{21}Sb_2SmNH_{16}$: Sm, 16.56; Sb, 28.45; C, 11.22; H, 1.88; N, 1.64. Found: Sm, 16.3; Sb, 28.7; C, 10.98; H, 1.82; N, 1.60. IR (KBr): 3341(br. s), 1632(s), 1599(s), 1471(s), 1386(s), 1318(m), 1294(s), 1126(s), 1071(m), 895(m), 740(m).

Preparation of $Eu(Sb_2L_2)(H_2O)_5(NO_3)\cdot H_2O$ (1D-Eu). **1D-Eu** was synthesized in the same way as **1D-La** except that $Eu(NO_3)_3\cdot 5H_2O$ was used instead of $La(NO_3)_3\cdot 6H_2O$. Colorless plate crystals of **1D-Eu** were obtained. Yield 42% based on $K_2Sb_2L_2$. Anal. Calcd for $C_8O_{21}Sb_2EuNH_{16}$: Eu, 17.72; Sb, 28.39; C, 11.20; H, 1.88; N, 1.63. Found: Eu, 17.5; Sb, 29.0; C, 11.04; H, 1.86; N, 1.60. IR (KBr): 3370(br. s), 1597(s), 1475(m), 1385(s), 1297(w), 1127(s), 1070(s), 895(m), 734(m).

Preparation of $Gd(Sb_2L_2)(H_2O)_5(NO_3)\cdot H_2O$ (1D-Gd). **1D-Gd** was synthesized in the same way as **1D-La** except that $Gd(NO_3)_3\cdot 6H_2O$ was used instead of $La(NO_3)_3\cdot 6H_2O$. Colorless plate crystals of **1D-Gd** were obtained. Yield 35% based on $K_2Sb_2L_2$. Anal. Calcd for $C_8O_{21}Sb_2GdNH_{16}$: Gd, 18.22; Sb, 28.22; C, 11.13; H, 1.87; N, 1.62. Found: Gd, 17.7; Sb, 27.4; C, 11.09; H, 1.79; N, 1.61. IR (KBr): 3357(br. s), 1635(m), 1599(s), 1476(s), 1388(s), 1297(s), 1126(s), 1070(s), 895(m), 733(m).

Preparation of $Tb(Sb_2L_2)(H_2O)_5(NO_3)\cdot H_2O$ (1D-Tb). An aqueous mixture (6.0 mL) containing $Tb(NO_3)_3\cdot 5H_2O$ (175.0 mg, 0.4 mmol) and $K_2Sb_2L_2$ (123.0 mg, 0.2 mmol) with pH ≈ 4 was placed in 16 mL vial, and the vial was sealed, heated to 90 °C under autogenous pressure for 72 h, and then cooled to room temperature at ambient atmosphere. The product was washed with deionized water and dried in air. Colorless plate crystals of **1D-Tb** were obtained. Yield 42% based on $K_2Sb_2L_2$. Anal. Calcd for $C_8O_{21}Sb_2TbNH_{16}$: Tb, 18.38; Sb, 28.16; C, 11.11; H, 1.87; N, 1.62. Found: Tb, 18.0; Sb, 27.3; C, 11.07; H, 1.79; N, 1.60. IR (KBr): 3394(br. s), 1630(w), 1598(s), 1475(w), 1385(s), 1320(w), 1295(s), 1128(s), 1070(m), 893(w), 739(m).

Preparation of $Dy(Sb_2L_2)(H_2O)_5(NO_3)\cdot H_2O$ (1D-Dy). **1D-Dy** was synthesized as in the same way as **1D-Tb** except that $Dy(NO_3)_3\cdot 5H_2O$ was used instead of $Tb(NO_3)_3\cdot 5H_2O$. A large amount of **1D-Dy** was obtained by evaporation of a filtrate of the reactant solution at ambient atmosphere. Yield 50% based on $K_2Sb_2L_2$. Anal. Calcd for $C_8O_{21}Sb_2DyNH_{16}$: Dy, 18.72; Sb, 28.05; C, 11.07; H, 1.86; N, 1.61. Found: Dy, 18.7; Sb, 28.8; C, 10.95; H, 1.96; N, 1.66. IR (KBr): 3394(br. s), 1630(w), 1600(s), 1478(m), 1382(w), 1315(w), 1293(s), 1125(m), 1071(m), 894(w), 742(w).

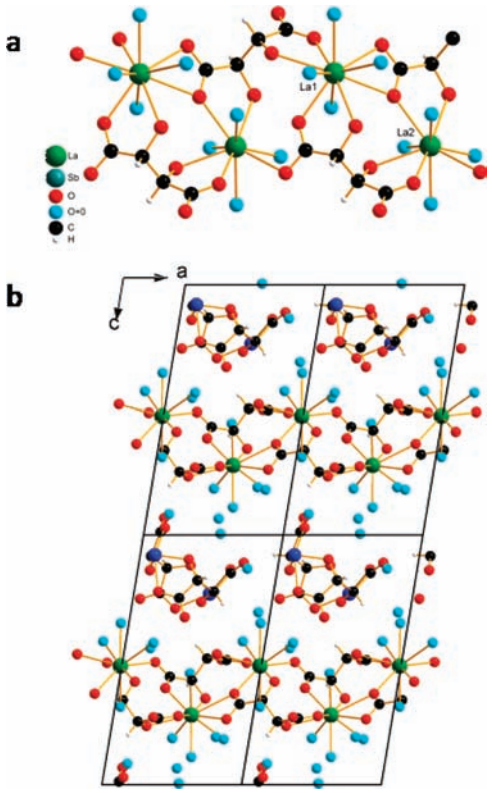

Figure 1. Ball-and-stick representation of **0D-La**: (a) coordination spheres of La1 and La2 and (b) view along the *b* axis showing the arrangement of chains and isolated dimers (Sb ions are blue).

Preparation of $Ho(Sb_2L_2)(H_2O)_5(NO_3)\cdot H_2O$ (1D-Ho). **1D-Ho** was synthesized in the same way as **1D-Dy** except that $Ho(NO_3)_3\cdot 5H_2O$ was used instead of $Dy(NO_3)_3\cdot 5H_2O$. Red plate crystals of **1D-Ho** were obtained. Yield 45% based on $K_2Sb_2L_2$. Anal. Calcd for $C_8O_{21}Sb_2HoNH_{16}$: Ho, 18.94; Sb, 27.97; C, 11.04; H, 1.85; N, 1.61. Found: Ho, 19.5; Sb, 27.6; C, 10.95; H, 1.75; N, 1.71. IR (KBr): 3408(br. s), 1628(s), 1595(s), 1476(s), 1379(s), 1316(m), 1288(m), 1123(s), 1072(m), 896(m), 740(m).

Preparation of $Er(Sb_2L_2)(H_2O)_5(NO_3)\cdot H_2O$ (1D-Er). **1D-Er** was synthesized in the same way as **1D-Dy** except that $Er(NO_3)_3\cdot 5H_2O$ was used instead of $Dy(NO_3)_3\cdot 5H_2O$. Red plate crystals of **1D-Er** were obtained. Yield 40% based on $K_2Sb_2L_2$. Anal. Calcd for $C_8O_{21}Sb_2ErNH_{16}$: Er, 19.16; Sb, 27.89; C, 11.00; H, 1.85; N, 1.60. Found: Er, 19.6; Sb, 25.5; C, 10.83; H, 1.75; N, 1.61. IR (KBr): 3421(br. s), 1632(w), 1598(s), 1474(m), 1376(m), 1277(s), 1067(m), 842(m), 768(w).

Preparation of $Tm(Sb_2L_2)(H_2O)_5(NO_3)\cdot H_2O$ (1D-Tm). **1D-Tm** was synthesized in the same way as **1D-Dy** except that $Tm(NO_3)_3\cdot 5H_2O$ was used instead of $Dy(NO_3)_3\cdot 5H_2O$. A few colorless needle crystals of **1D-Tm** suitable for single-crystal X-ray diffraction were obtained.

Preparation of $Yb(Sb_2L_2)(H_2O)_5(NO_3)\cdot H_2O$ (1D-Yb). An aqueous mixture (6.0 mL) containing $Yb(NO_3)_3\cdot 5H_2O$ (270.0 mg, 0.6 mmol) and $K_2Sb_2L_2$ (123.0 mg, 0.2 mmol) with a pH ≈ 3 was placed in a 16 mL vial, and the vial was sealed, heated to 90 °C under autogenous pressure for 72 h, and then cooled to room temperature at ambient atmosphere. A few colorless needle crystals of **1D-Yb** suitable for single-crystal X-ray diffraction were obtained by evaporation of filtrate from the reaction mixture.

Preparation of $Lu(Sb_2L_2)(H_2O)_5(NO_3)\cdot H_2O$ (1D-Lu). **1D-Lu** was synthesized in the same way as **1D-Yb** except $Lu(NO_3)_3$ was used in place of $Yb(NO_3)_3\cdot 5H_2O$. A few colorless needle crystals of **1D-Lu** suitable for single-crystal X-ray diffraction were obtained.

Preparation of $Y(Sb_2L_2)(H_2O)_5(NO_3)\cdot H_2O$ (1D-Y). **1D-Y** was synthesized in the same way as **1D-Yb** except $Y(NO_3)_3\cdot 6H_2O$ was used in place of $Yb(NO_3)_3\cdot 5H_2O$. A few colorless needle crystals of **1D-Y** suitable for single-crystal X-ray diffraction were obtained.

Preparation of $[(La(H_2O)_5)_2(Sb_2L_2)_3]\cdot 5H_2O$ (2D(I)-La). A mixture containing $La(NO_3)_3\cdot 6H_2O$ (44.0 mg, 0.1 mmol), $K_2Sb_2L_2$ (92.0 mg, 0.15 mmol), H_2O (3 mL), and EtOH (2 mL) with pH ≈ 4 was placed in a 16 mL vial, and the vial was sealed, heated to 95 °C under autogenous pressure for 72 h, and then cooled to room temperature at ambient atmosphere. The product was washed with deionized water and dried in air. Colorless plate crystals of **2D(I)-La** were obtained. Yield 42% based on $K_2Sb_2L_2$. Anal. Calcd for $C_{24}O_{51}Sb_6La_2H_{42}$: La, 12.89; Sb, 33.90; C, 13.38; H, 1.96. Found: La, 12.7; Sb, 34.5; C, 13.29; H, 1.88. IR (KBr): 3394(br. s), 1613(s), 1374(s), 1125(s), 1071(m), 897(w), 734(m).

Preparation of $[(Ce(H_2O)_5)_2(Sb_2L_2)_3]\cdot 5H_2O$ (2D(I)-Ce). **2D(I)-Ce** was synthesized in the same way as **2D(I)-La** except that $Ce(NO_3)_3\cdot 6H_2O$ was used instead of $La(NO_3)_3\cdot 6H_2O$. Colorless plate crystals of **2D(I)-Ce** were obtained. Yield 40% based on $K_2Sb_2L_2$. Anal. Calcd for $C_{24}O_{51}Sb_6Ce_2H_{42}$: Ce, 12.99; Sb, 33.86; C, 13.36; H, 1.96. Found: Ce, 13.1; Sb, 33.6; C, 13.28; H, 1.87. IR (KBr): 3402(br. s), 1615(s), 1373(s), 1125(s), 1071(m), 895(m), 732(m).

Preparation of $[(Pr(H_2O)_5)_2(Sb_2L_2)_3]\cdot 5H_2O$ (2D(I)-Pr). **2D(I)-Pr** was synthesized in the same way as **2D(I)-La** except that $Pr(NO_3)_3\cdot 6H_2O$ was used instead of $La(NO_3)_3\cdot 6H_2O$. Green plate crystals of **2D(I)-Pr** were obtained. Yield 50% based on $K_2Sb_2L_2$. Anal. Calcd for $C_{24}O_{51}Sb_6Pr_2H_{42}$: Pr, 13.05; Sb, 33.84; C, 13.35; H, 1.96. Found: Pr, 13.7; Sb, 33.4; C, 13.42; H, 1.94. IR (KBr): 3394(br. s), 1608(s), 1375(s), 1126(s), 1071(m), 896(m), 733(m).

Preparation of $[(La(H_2O)_5)_2(Sb_2L_2)_3]\cdot 6H_2O$ (2D(II)-La). A mixture containing $La(NO_3)_3\cdot 6H_2O$ (88.0 mg, 0.2 mmol), $K_2Sb_2L_2$ (124.0 mg, 0.2 mmol), H_2O (2 mL), and glycol (4 mL) with pH ≈ 4 was placed in a 16 mL vial, and the vial was sealed, heated to 100 °C under autogenous pressure for 120 h, and then cooled to room temperature at ambient atmosphere. The product was washed with deionized water and dried in air. A few colorless plate crystals of **2D(II)-La** were obtained.

RESULTS AND DISCUSSION

Synthesis. All compounds were synthesized under hydrothermal conditions at 90−100 °C. In order to optimize phase purities and yields, different solvents were used, such as pure water, water and ethanol, and water and glycol. **0D-La** was originally obtained by hydrothermal reaction of $La(NO_3)_3$, $K_2Sb_2L_2$, HCOOH, and HCOOK in water. The coordinated tartrate ligands were generated from the decomposition of $K_2Sb_2L_2$. In fact, some small octahedral colorless crystals were found in the product, and the single-crystal X-ray study revealed that these small crystals were Sb_2O_3. Thus, we modified the synthesis by addition of a stoichiometric amount of L-tartaric acid into the reaction; pure **0D-La** samples were then obtained. In the other syntheses the $Sb_2L_2^{2-}$ units remained intact. We deduced that the decomposition of $Sb_2L_2^{2-}$ units in the reaction may be attributed to the presence of HCOOH and HCOOK, which is frequently used as buffering solution to control the pH. It is noteworthy that in the syntheses of whole **1D-Ln** series from La to Lu, the synthesis conditions increase in severity. From **1D-La** to **1D-Gd**, the synthesis conditions were identical, the reactants were mixed stoichiometrically, and pure crystals were harvested directly after the reactions cooled down. From **1D-Tb** to **1D-Tm**, the amount of $Ln(NO_3)_3$ had to be doubled to get the

dx.doi.org/10.1021/ic201274c |*Inorg. Chem.* 2011, 50, 9073–9082

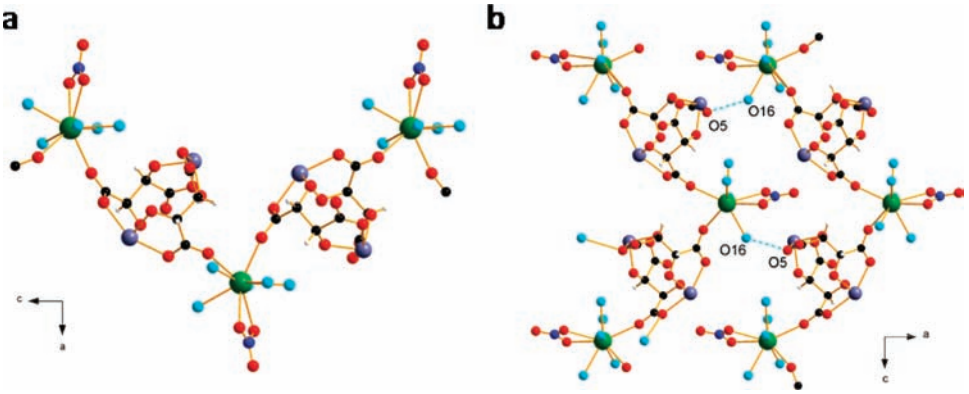

Figure 2. Ball-and-stick representation of **1D-Ln**: (a) a single chain and (b) view along the *b* axis showing two chains hydrogen bonded to form layers in the *ac* plane.

products. Only **1D-Tb** could be obtained directly, the other four products could only be obtained by evaporation of the filtrates, and the yields decreased from **1D-Dy** to **1D-Tm**. For **1D-Yb** and **1D-Lu**, the amount of $Ln(NO_3)_3$ had to be tripled and only a few crystals could be produced by evaporation of the filtrates. This trend is related to the decrease in ionic radius from La to Lu. The coordination number of Ln in **1D-La** is nine; therefore, the steric crowding in the coordination sphere increases from **1D-La** to **1D-Lu**. This provides some guidelines for syntheses of isostructural compounds of the whole lanthanide series. For **2D(I)-Ln** series, only compounds with the first three large Ln ions were synthesized; this is probably also due to the steric hindrance. Though the lanthanide ions are nine coordinated as are those in the **1D-Ln** compound, the steric crowding is more severe, because two more oxygen atoms in the coordination spheres are provided by two $Sb_2L_2^{2-}$ units, compared to the **1D-Ln** structure. This may explain why only the first three **2D(I)-Ln** compounds could be obtained.

Crystal Structures. The coordination of L-tartrate acid and $Sb_2L_2^{2-}$ secondary building units is shown in Figure S2, Supporting Information. The following structure discussions are based on the CIF files. The formulas are further confirmed by elemental analyses (EA) and TG studies. The phase purities were checked by XRD (Figure S4, Supporting Information).

$[La(H_2L)(H_2O)_4]_2[Sb_2L_2]\cdot 5H_2O$ (***0D-La***). Only one compound with the 0D structure, **0D-La**, was obtained. It crystallizes in space group *P*1. There are two crystallographically different La^{3+} ions, two tartrate ligands, and one $Sb_2L_2^{2-}$ unit in the asymmetric unit. Both La^{3+} ions are coordinated by 10 oxygen atoms, 6 of them are from 3 tartrate ligands; 4 water molecules complete the coordination spheres in dodecahedron geometry (Figure 1a). The bond lengths range from 2.517(8) to 2.770(7) Å for La(1) and from 2.523(7) to 2.903(8) Å for La(2). The two tartrate ligands, with all carboxylate groups deprotonated, share similar coordination modes: each carboxylate group chelates to one La^{3+} ion.

One oxygen atom from the carboxylate group further coordinates to a third La^{3+} ion together with one oxygen atom from adjacent hydroxyl group (Figure S2(a), Supporting Information). In this way, the ligands connect La^{3+} ions into a chain along the *a* axis (Figure 1b). The chains are further assembled into 2D layers in the *ab* plane by hydrogen bonds with O···O distances ranging from 2.713 to 2.927 Å. Isolated $Sb_2L_2^{2-}$ units reside between layers and form hydrogen bonds with the

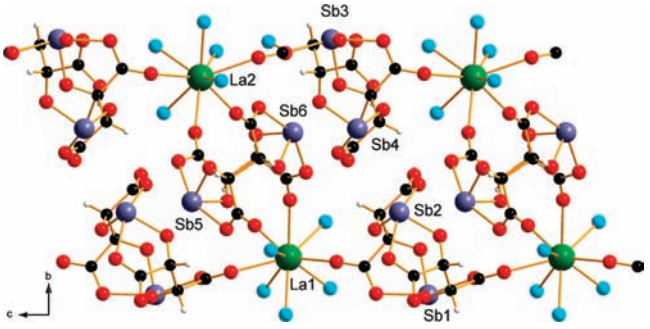

Figure 3. Ball-and-stick representation of **2D(I)-La**. View of the layer along the *a* axis.

layers from both sides (the O···O distances range from 2.817 to 2.888 Å). Also, the $Sb_2L_2^{2-}$ uints are aligned along the *b* axis with very weak interactions between Sb2—O13 (Sb···O distance 2.962 Å).[18] Lattice water molecules hydrogen bond to layers as well as to $Sb_2L_2^{2-}$ units (Figures 1b and S3, Supporting Information).

$La(Sb_2L_2)(H_2O)_5(NO_3)\cdot H_2O$ (***1D-La***). The whole series of 1D structures was synthesized (Ln = La—Lu or Y, except Pm) and represents the first example of homochiral lanthanide structures that can be formed throughout the whole lanthanide series. Here, we only describe the structure of **1D-La**. **1D-La** crystallizes as a one-dimensional homochiral coordination polymer in space group $P2_12_12_1$. As illustrated in Figure 2, each La^{3+} ion is coordinated by two oxygen atoms from two distinct $Sb_2L_2^{2-}$ units, two oxygen atoms from one nitrate anion, and five water molecules, in a tricapped trigonal prism motif. The La—O bond lengths vary from 2.444(4) to 2.656(4) Å, shorter than those in **0D-La**. Each $Sb_2L_2^{2-}$ unit uses two out of four free oxygen atoms from two different tartrate ligands to coordinate to two La^{3+} ions (Figure S2(b), Supporting Information), and these two oxygen atoms are from the two carboxylate groups that coordinate to one Sb^{3+} ion. The $Sb_2L_2^{2-}$ units thus connect the La^{3+} ions into a chiral zigzag chain with 2_1 screw axis along *c*. The helices extend along the *a* axis through hydrogen bonding between O16w and O5 (O···O distances 2.772 Å) to form layers in the *ac* plane (Figure 2b).

The layers are connected to other layers from above and below through several hydrogen bonds (the O···O distances ranging from 2.728 to 2.891 Å), leading to a 3D supramolecular network;

dx.doi.org/10.1021/ic201274c |*Inorg. Chem.* 2011, 50, 9073–9082

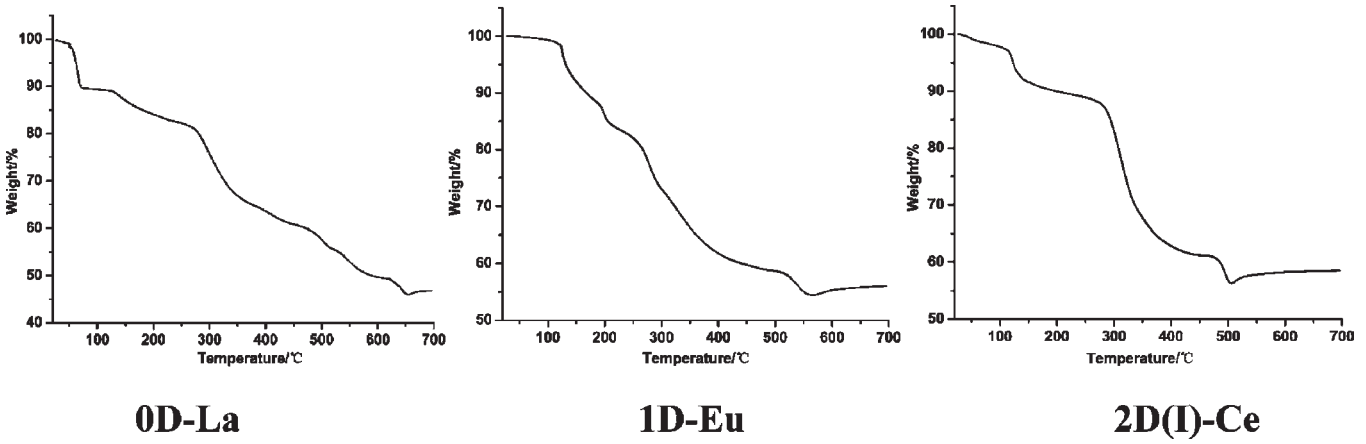

Figure 4. Thermogravimetric analysis data for **0D-La**, **1D-Eu**, and **2D(I)-Ce**.

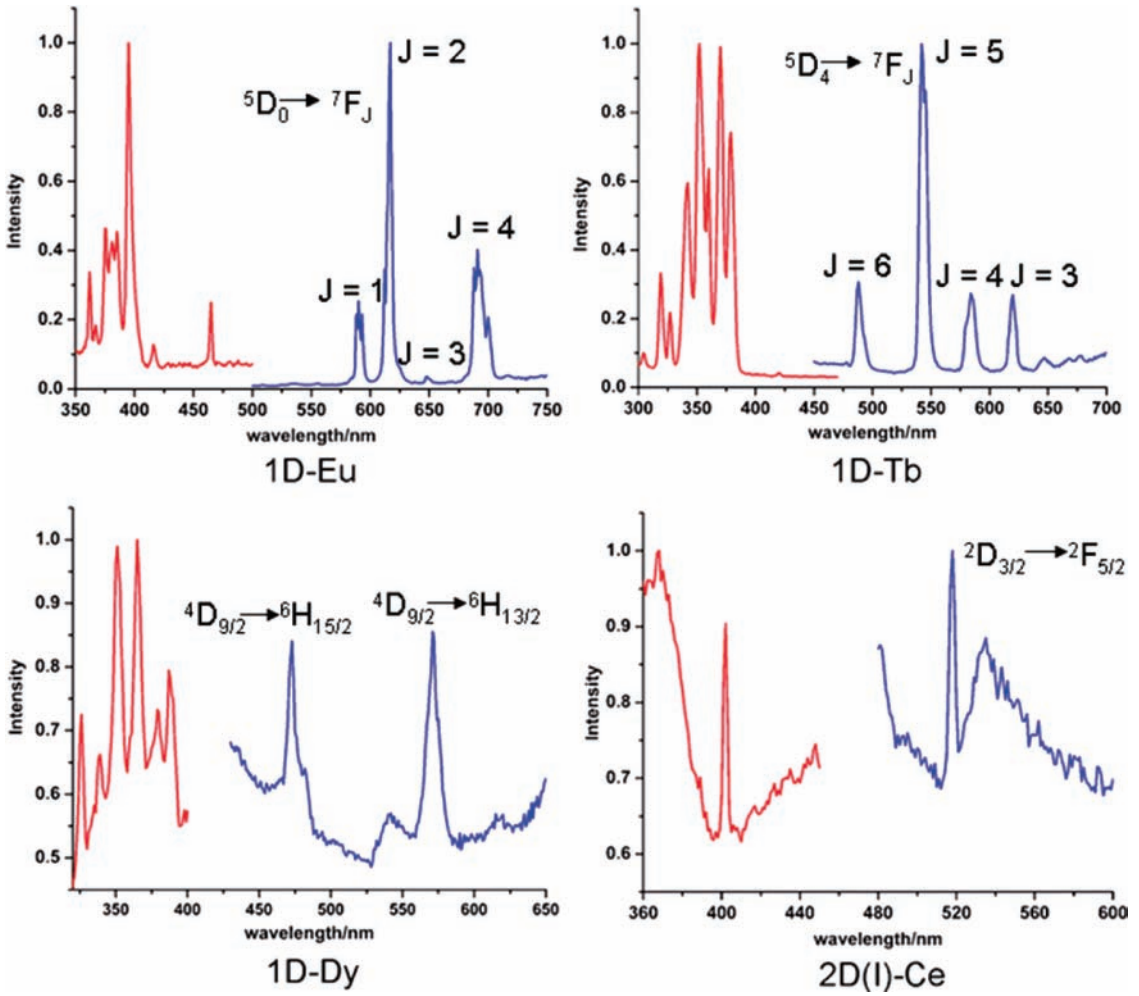

Figure 5. Solid-state photoluminescence spectra of **1D-Eu**, **1D-Tb**, **1D-Dy**, and **2D(I)-Ce** at room temperature. Red lines present excitation spectra; blue lines show emission spectra.

lattice water molecules (O21w) reside in the voids between the layers.

[(La(H$_2$O)$_5$)$_2$(Sb$_2$L$_2$)$_3$]·5H$_2$O (***2D(I)-La***). Three compounds were obtained (Ln = La, Ce, Pr) in this series. The structure of **2D(I)-La** is described here. As indicated by single-crystal X-ray diffraction, the compound crystallizes in space group $P2_1$. There are two crystallographically different La^{3+} ions (La(1) and La(2)) and three $Sb_2L_2^{2-}$ units ($Sb_2L_2^{2-}$(I) [Sb(1),Sb(2)], $Sb_2L_2^{2-}$(II) [Sb(3),Sb(4)], $Sb_2L_2^{2-}$(III) [Sb(5),Sb(6)]) in the asymmetric unit (Figure 3). La(1) is surrounded by nine

dx.doi.org/10.1021/ic201274c |*Inorg. Chem.* 2011, 50, 9073–9082

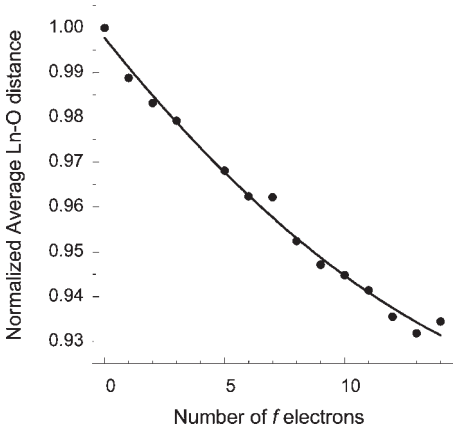

Figure 6. Variation of the average Ln−O bond length in **1D-Ln** with the number of f electrons; the solid line is a quadratic fit to the data.

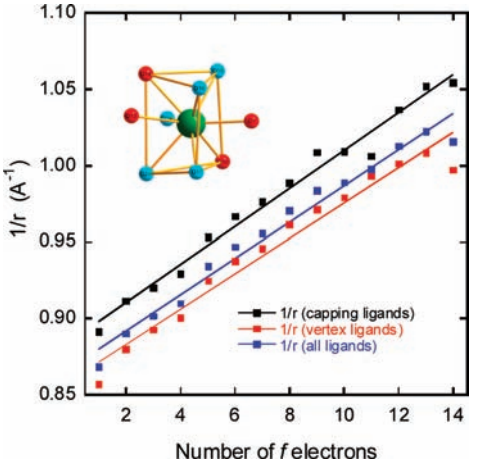

Figure 7. Variation of the inverse of the lanthanide ion radius calculated from the Ln−O bond lengths.

oxygen atoms, with two oxygen atoms from two $Sb_2L_2^{2-}$(I) units and two oxygen atoms from two $Sb_2L_2^{2-}$(III) units, and the remaining are five water molecules (Figure 3), which gives rise to a tricapped trigonal prism motif.

The coordination sphere of La(2) is similar to that of La(1), except that two $Sb_2L_2^{2-}$(II) units, rather than $Sb_2L_2^{2-}$(I), provide two oxygen atoms. The La−O bond lengths range from 2.467(4) to 2.672(4) Å for La(1) and from 2.486(4) to 2.619(4) Å for La(2), a little longer than those in **1D-La** and shorter than those in **0D-La**. $Sb_2L_2^{2-}$(I) and $Sb_2L_2^{2-}$(II) units both use two of the four free oxygen atoms to coordinate La^{3+} ions, as found in **1D-Ln**, while for the $Sb_2L_2^{2-}$(III) unit all four free oxygen atoms connect La(1) and La(2) ions in a severely distorted tetrahedron motif (Figure S2(c), Supporting Information). $Sb_2L_2^{2-}$(I) and $Sb_2L_2^{2-}$(II) units connect La(1) and La(2) ions into 1D helices along the [001] and [101] directions, respectively (Figure 3). The helices are slightly different from those in **1D-La**. The helices in **2D(I)-La** are straight chains, while in **1D-La** they are zigzag chains. The difference arises from steric crowding from the two coordinated $Sb_2L_2^{2-}$(III) units, which link these two types of helices into infinite slabs, with each $Sb_2L_2^{2-}$(III) unit linked to two La(1) helices and two La(2) helices. The slabs then stack along the *b* axis; lattice water molecules are located within and between the slabs. The structure of **2D(II)-La** is almost the same as that of **2D(I)-La**. It crystallizes in the higher symmetry space group *C*2 and contains only one-half of the atoms in the asymmetric unit compared to **2D(I)-La**. There is one more lattice water molecule in the unit, which might cause the change of space group from $P2_1$ to *C*2.

Thermogravimetric Analysis. The thermal stabilities were investigated, and the results are shown in Figure 4. **0D-La** loses the lattice water molecules up to 72 °C (calcd 9.16%, found 9.92%); then it is stable up to 124 °C. Above this temperature the framework decomposes in a series of steps to give a residue of La_2O_3, and Sb_2O_3 (calcd 44.9%, found 45.9%). **1D-Eu** is stable up to 100 °C; then it loses weight gradually in a series of steps without well-defined intermediate plateaus to give a residue of Eu_2O_3 and Sb_2O_3 (calcd 54.5%, found 54.4%). **2D(I)-Ce** also shows a gradual weight loss without well-defined intermediate plateaus to give a residue of Ce_2O_3 and Sb_2O_3 (calcd 55.8%, found 56.3%).

Photoluminescence Measurements. The photoluminescence spectra of **1D-Eu**, **1D-Tb**, **1D-Dy**, and **2D(I)-Ce** were recorded in the solid state at room temperature. The photoluminescence spectrum of $K_2Sb_2L_2$ was also recorded, which displays a weak emission at 450 nm when excited at 348 nm (Figure S5, Supporting Information). As illustrated in Figure 5, for **1D-Eu**, the emission spectrum arises from the transitions of $^5D_0 \rightarrow {}^7F_J$ (J = 1, 2, 3, 4). The corresponding emission peaks are 590, 617, 648, and 691 nm, respectively, when excited at 400 nm. For **1D-Tb**, upon excitation at 370 nm, the spectrum shows four emission bands at 488, 542, 584, and 620 nm corresponding to transitions $^5D_4 \rightarrow {}^7F_J$ (J = 6, 5, 4, 3). The most intensive emissions are at 617 and 542 nm for **1D-Eu** and **1D-Tb**, respectively. The emission spectrum for **1D-Dy** exhibits two bands at 486 and 576 nm with similar intensities upon excitation at 365 nm. They are attributed to the transitions of $^4F_{9/2} \rightarrow {}^6H_{15/2}$ and $^4F_{9/2} \rightarrow {}^6H_{13/2}$. A weak emission band at 520 nm was observed for **2D(I)-Ce**, upon excitation at 400 nm, which could be assigned to the transition $^2D_{3/2} \rightarrow {}^5F_{5/2}$.

Because all the compounds are noncentrosymmetric, their nonlinear optical (NLO) properties were checked. Second-harmonic generation (SHG) could be observed only for **1D-Tb** with an efficiency comparable to that of α-quartz.

Lanthanide Contraction Investigation. The lanthanide contraction is a well-known phenomenon that has been recently revisited. Two models have been proposed: a quadratic dependence of the decrease of certain parameters such as Ln−X bond lengths[15b] and a linear dependence of the inverse of the experimentally determined lanthanide ionic radii, both vs the number of f electrons.[15c] As we obtained a complete series of **1D-Ln** structures, we tested both models with our experimental data.

Ln−O Bond Lengths. All Ln−O bond lengths are listed in Table S1, Supporting Information, and they are plotted vs the number of f electrons in Figure S5, Supporting Information. The decrease for each bond length varies significantly (2.3−9.6%) from La to Lu. The variation is much larger than reported by Seitz at al. (6.6−8.6%) for lanthanide complexes with the ligand TREN-1,2-HOIQO.[15b] The difference is due to different coordination numbers and coordination modes. The Ln^{3+} ions in **lD-Ln** series are nine coordinated, and the highest denticity is 2 from the nitrate anion. The higher coordination number may cause less uniformity in the trend, while the lower denticity can grant each bond more freedom to change. However, the sum of the Ln−O bond lengths decreases by 7.0%, similar to that

dx.doi.org/10.1021/ic201274c |*Inorg. Chem.* 2011, 50, 9073–9082

reported by Seitz et al. (7.6%) and also in accordance with typical values for the lanthanide contraction. The decrease in length of an individual bond does not show a second-order polynomial dependence. The sum of individual Ln−O bond lengths averages out the individual deviations and is well fit by a second-order polynomial (Figure 6). The fitting results are given in Table S3, Supporting Information, and agree with the results in the literature.[15a,b]

Ionic Radius. Recently, Raymond et al. proposed that the lanthanide contraction could be described by a linear relation between the inverse of ionic radius and the number of f electrons:[15c] $1/r(x) = a + bx$, where x is the number of f electrons in the lanthanide ion of interest and $r(x)$ values are obtained by subtracting the ionic radius of oxygen (1.4 Å)[19] from the Ln−O internuclear distances. In the **1D-Ln** series, all nine Ln−O bond lengths are different. They are treated in three different ways: the sum, vertex oxygen atoms, and capping oxygen atoms. The results are shown in Figure 7 and Table S4, Supporting Information. Good linear fits were obtained even for Tm and Yb. The linear fits almost parallel each other. This means that in the **1D-Ln** series the trends revealed by three sets of data are almost the same, which is quite different from the results from the literature.[15c]

CONCLUSION

In summary, by utilizing a chiral dimer ligand $Sb_2L_2^{2-}$ as a secondary building unit, three series of homochiral compounds from 0D to 2D were synthesized. The ligand presents two different types of coordination modes. The fluorescence properties were studied for certain compounds, which display characteristic emissions. Second-order nonlinear measurements indicate that **1D-Tb** has a SHG efficiency that is comparable with α-quartz. The lanthanide contraction was investigated for the first series of isostructural homochiral lanthanide compounds (Ln = La−Lu, except Pm, or Y) by fitting the Ln−O bond lengths, O−O distances, and the inverse of ionic radii with two different models. Further studies of the coordination chemistry of the chiral antimony dimer ligand are ongoing.

ASSOCIATED CONTENT

Supporting Information. X-ray crystallographic data in CIF format, additional structure figures, XRD patterns, photoluminescence data, lanthanide contraction figures, and fitting results in PDF format. This material is available free of charge via the Internet at http://pubs.acs.org.

AUTHOR INFORMATION

Corresponding Author

*Phone: 713-743-2785. Fax: 713-743-2787. E-mail: ajjacob@uh.edu.

ACKNOWLEDGMENT

We thank the R. A. Welch Foundation (#E-0024) for support of this work.

REFERENCES

(1) (a) Eddaoudi, M.; Kim, J.; Rosi, N.; Vodka, D.; Wachter, J.; O'Keeffe, M.; Yaghi, O. M. *Science* **2002**, *295*, 469. (b) Matsuda, R.; Kitaura, R.; Kitagawa, S.; Kubota, Y.; Belosludov, R. V.; Kobayashi, T. C.; Salamoto, H.; Chiba, T.; Takata, M.; Kawazoe, Y.; Mita, Y. *Nature* **2005**, *436*, 238. (c) Wu, C. D.; Lin, W. B. *Angew. Chem., Int. Ed.* **2005**, *44*, 1958. (d) Sun, D. F.; Ma, S. Q.; Ke, Y. X.; Collins, D. J.; Zhou, H. C. *J. Am. Chem. Soc.* **2006**, *128*, 3896. (e) Wang, X. Q.; Liu, L. M.; Jacobson, A. J. *Angew. Chem., Int. Ed.* **2006**, *45*, 6499. (f) Zhu, A. X.; Lin, J. B.; Zhang, J. P.; Chen, X. M. *Inorg. Chem.* **2009**, *48*, 3882.

(2) (a) Yoshizawa, M.; Tamura, M.; Fujita, M. *Science* **2006**, *312*, 251. (b) Dang, D. B.; Bai, Y.; He, C.; Wang, J.; Duan, C. Y.; Niu, J. Y. *Inorg. Chem.* **2010**, *49*, 1280.

(3) (a) Xiang, S. C.; Wu, X. T.; Zhang, J. J.; Fu, R. B.; Hu, S. M.; Zhang, X. D. *J. Am. Chem. Soc.* **2005**, *127*, 16352. (b) Prins, F.; Pasca, E.; Jongh, L. J. D.; Kooijman, H.; Spek, A. L.; Tanase, S. *Angew. Chem., Int. Ed.* **2007**, *46*, 6081. (c) Yang, T. H.; Knowles, E. S.; Pajerowski, D. M.; Xia, J. S.; Yin, L.; Gao, S.; Meisel, M. W.; Zheng, L. M. *Inorg. Chem.* **2010**, *49*, 8474.

(4) (a) Pang, J.; Marcotte, E. J. P.; Seward, C.; Brown, R. S.; Wang, S. N. *Angew. Chem., Int. Ed.* **2001**, *40*, 4042. (b) Huang, Y. G.; Wu, B. L.; Yuan, D. Q.; Xu, Y. Q.; Jiang, F. L.; Hong, M. C. *Inorg. Chem.* **2007**, *46*, 1171. (c) Jhang, P. C.; Chuang, N. T.; Wang, S. L. *Angew. Chem., Int. Ed.* **2010**, *49*, 4200. (d) Pramanik, S.; Zheng, C.; Zhang, X.; Emge., T. J.; Li, J. *J. Am. Chem. Soc.* **2011**, *133*, 4153.

(5) (a) Chen, J.-X.; Tang, X.-Y.; Chen, Y.; Zhang, W.-H.; Li, L.-L.; Yuan, R.-X.; Zhang, Y.; Lang, J.-P. *Cryst. Growth Des.* **2009**, *9*, 1461. (b) Wang, X. Q.; Liu, L. M.; Makarenko, T.; Jacobson, A. J. *Cryst. Growth Des.* **2010**, *10*, 3752. (c) He, H. Y.; Yuan, D. Q.; Ma, H. Q.; Sun, D. F.; Zhang, G. Q.; Zhou, H. C. *Inorg. Chem.* **2010**, *49*, 7605.

(6) (a) Montgomery, C. P.; Parker, D.; Lamarque, L. *Chem. Commun.* **2007**, 3841. (b) Soares-Santos, P. C. R.; Cunha-Silva, L.; Paz, F. A. A.; Ferreira, R. A. S.; Rocha, J.; Carlos, L. D.; Nogueira, H. I. S. *Inorg. Chem.* **2010**, *49*, 3428. (c) Bernot, K.; Luzon, J.; Bogani, L.; Etienne, M.; Sangregorio, C.; Shanmugam, M.; Caneschi, A.; Sessoli, R.; Gatteschi, D. *J. Am. Chem. Soc.* **2009**, *131*, 5573. (d) Rinck, J.; Novitchi, G.; Heuvel, W. V. D.; Ungur, L.; Lan, Y. H.; Wernsdorfer, W.; Anson, C. E.; Chibotaru, L. F.; Powell, A. K. *Angew. Chem., Int. Ed.* **2010**, *49*, 7583. (e) Guo, F. S.; Liu, J. L.; Leng, J. D.; Meng, Z. S.; Lin, Z. J.; Tong, M. L.; Gao, S.; Ungur, L.; Chibotaru, L. F. *Chem.—Eur. J.* **2011**, *17*, 2458. (f) Dang, D. B.; Wu, P. Y.; He, C.; Zhong, X.; Duan, C. Y. *J. Am. Chem. Soc.* **2010**, *132*, 14321. (g) Belousoff, M. J.; Ung, P.; Forsyth, C. M.; Tor, Y.; Spiccia, L.; Graham, B. *J. Am. Chem. Soc.* **2009**, *131*, 1106. (f) De Lill, D. T.; De Bettencourt-Dias, A.; Cahill, C. L. *Inorg. Chem.* **2007**, *46*, 3970. (g) Wang, X. L.; Li, L. C.; Liao, D. Z. *Inorg. Chem.* **2010**, *49*, 4735.

(7) (a) Lee, W. R.; Ryu, A. W.; Lee, J. W.; Yoon, J. H.; Koh, E. K.; Hong, C. S. *Inorg. Chem.* **2010**, *49*, 4723. (b) Guo, X. D.; Zhu, G. S.; Li, Z. Y.; Chen, Y.; Li, X. T.; Qiu, S. L. *Inorg. Chem.* **2006**, *45*, 4065.

(8) (a) Seo, J. S.; Whang, D.; Lee, H.; Jun, S. I.; Oh, J.; Jeon, Y. J.; Kim, K. *Nature* **2000**, *404*, 982. (b) Bradshaw, D.; Prior, T. J.; Cussen, E. J.; Claridge, J. B.; Rosseinsky, M. J. *J. Am. Chem. Soc.* **2004**, *126*, 6106. (c) Wezenberg, S. J.; Salassa, G.; Escudero-Adán, E. C.; Benet-Buchholz, J.; Kleij, A. W. *Angew. Chem., Int. Ed.* **2011**, *50*, 713. (d) Li, G.; Yu, W. B.; Cui, Y. *J. Am. Chem. Soc.* **2008**, *130*, 4582.

(9) (a) Liang, X. Q.; Li, D. P.; Li, C. H.; Zhou, X. H.; Li, Y. Z.; Zuo, J. L.; You, X. Z. *Cryst. Growth Des.* **2010**, *10*, 2596. (b) Zhang, W.; Ye, H. Y.; Xiong, R. G. *Coord. Chem. Rev.* **2009**, *253*, 2980. (c) Xiao, F. P.; Hao, J.; Zhang, J.; Lv, C. L.; Yin, P. C.; Wang, L. S.; Wei, Y. G. *J. Am. Chem. Soc.* **2010**, *132*, 5956.

(10) (a) Qin, J.; Qin, C.; Wang, X. L.; Wang, E. B.; Su, Z. M. *Chem. Commun.* **2010**, 604. (b) Xi, X. B.; Fang, Y.; Dong, T. W.; Cui, Y. *Angew. Chem., Int. Ed.* **2011**, *50*, 1154. (c) Zhang, Z. M.; Yao, S.; Li, Y. G.; Clérac, R.; Lu, Y.; Su, Z. M.; Wang, E. B. *J. Am. Chem. Soc.* **2009**, *131*, 14600. (d) Marino, N.; Armentano, D.; Mastropietro, T. F.; Julve, M.; Lloret, F.; Munno, G. D. *Cryst. Growth Des.* **2010**, *10*, 1757. (e) Gedrich, K.; Senkovska, I.; Baburin, I. A.; Mueller, U.; Trapp, O.; Kaskel, S. *Inorg. Chem.* **2010**, *49*, 4440.

(11) (a) Zhang, J.; Chen, S. M.; Nieto, R. A.; Wu, T.; Feng, P. Y.; Bu, X. H. *Angew. Chem., Int. Ed.* **2010**, *49*, 1267. (b) Zhang, J.; Chen, S. M.; Wu, T.; Feng, P. Y.; Bu, X. H. *J. Am. Chem. Soc.* **2008**, *130*, 12882.

(12) (a) Lan, Y. Q.; Li, S. L.; Su, Z. M.; Shao, K. Z.; Ma, J. F.; Wang, X. L.; Wang, E. B. *Chem. Commun* **2008**, 58. (b) Johansson, A.;

Håkansson, M.; Jagner, S. *Chem.—Eur. J.* **2005**, *11*, 5311. (c) Gao, E. Q.; Bai, S. Q.; Wang, Z. M.; Yan, C. H. *J. Am. Chem. Soc.* **2003**, *125*, 4984.

(13) (a) Yeung, H. H. M.; Kosa, M.; Parrinello, M.; Forster, P. M.; Cheetham, A. K. *Cryst. Growth Des.* **2011**, *11*, 221. (b) Appelhans, L. N.; Kosa, M.; Radha, A. V.; Simoncic, P.; Navrotsky, A.; Parrinello, M.; Cheetham, A. K. *J. Am. Chem. Soc.* **2009**, *131*, 15375. (c) Kam, K. C.; Young, K. L. M.; Cheetham, A. K. *Cryst. Growth Des.* **2007**, *7*, 1522. (d) Patil, H. M.; Sawant, D. K.; Bhavsar, D. S.; Patil, J. H.; Girase, K. D. *Arch. Phys. Res.* **2011**, *2*, 239. (e) Labutina, M. L.; Marychev, M. O.; Portnov, V. N.; Somov, N. V.; Chuprunov, E. V. *Crystallogr. Rep.* **2011**, *56*, 72. (f) Kaizaki, S.; Kato-Igawa, Y.; Tsukuda, T.; Nakano, M. *J. Coord. Chem.* **2010**, *63*, 967. (g) Rood, J A.; Noll, B. C.; Henderson, K. W. *J. Solid State Chem.* **2010**, *183*, 270. (h) Rodrigues, E. C.; Carvalho, C. T.; De Siqueira, A. B.; Bannach, G.; Ionashiro, M. *Thermochim. Acta* **2009**, *496*, 156. (i) Coronado, E.; Galán-Mascarós, J. R.; Gómez-García, C. J.; Murcia-Martínez, A. *Chemistry—Eur. J.* **2006**, *12*, 3484.

(14) (a) Gress, M. E.; Jacobson, R. A. *Inorg. Chim. Acta* **1974**, *8*, 209. (b) Sagatys, D. S.; Smith, G.; Lynch, D. E.; Kennard, C. H. L. *J. Chem. Soc., Dalton Trans.* **1991**, 361. (c) Bohatý, L.; Fröhlich, R.; Tebbe, K.-F. *Acta Crystallogr.* **1983**, *C39*, 59. (d) Palenik, R. C.; Abboud, K. A.; Palenik, G. J. *Inorg. Chim. Acta* **2005**, *358*, 1034.

(15) (a) Quadrelli, E. A. *Inorg. Chem.* **2002**, *41*, 167. (b) Seitz, M.; Oliver, A. G.; Raymond, K. N. *J. Am. Chem. Soc.* **2007**, *129*, 11153. (c) Raymond, K. N.; Wellman, D. L.; Sgarlata, C.; Hill, A. P. *C. R. Chim.* **2010**, *13*, 849. (d) Zehnder, R. A.; Clark, D. L.; Scott, B. L.; Donohoe, R. J.; Palmer, P. D.; Runde, W. H.; Hobart, D. E. *Inorg. Chem.* **2010**, *49*, 4781.

(16) (a) Kustaryono, D.; Kerbellec, N.; Calvez, G.; Freslou, S.; Daiguebonne, C.; Guillou, O. *Cryst. Growth Des.* **2010**, *10*, 775. (b) Gerkin, R. E.; Reppart, W. J. *Acta Crystallogr.* **1984**, *C40*, 781.

(17) Sheldrick, G. M. *SHELXTL, Program for Refinement of Crystal Structures*; Siemens Analytical X-ray Instruments: Madison, WI, 1994.

(18) Menchetti, S.; Sabelli, C. *Am. Mineral.* **1980**, *65*, 940.

(19) Shannon, R. D. *Acta Crystallogr.* **1976**, *A32*, 751.